Angewandte Chemie
Eine Zeitschrift der Gesellschaft Deutscher Chemiker

Supporting Information

69451 Weinheim, Germany

Supporting information for Liedl, Olapinski & Simmel

1. Materials and Methods

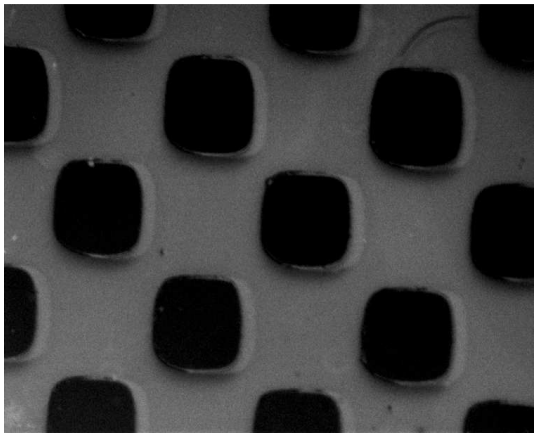

Figure 1: Binding of thiol-labeled DNA to a patterned, but transparent surface: A Au pattern was defined on a glass coverslip with standard lithography techniques. Then the sample was sputtered with Ar ions until no pattern was visible anymore. The modified surface was exposed to a DNA strand labeled with a dye on one end and a thiol-group on the other end. The pattern is revealed again under a fluorescence microscope. The side-length of the squares is 50μm

Chemicals:
Unless stated otherwise, all chemicals were purchased from Sigma-Aldrich, Germany. The DNA strand M with the sequence 5' - CCC TAA CCC TAA CCC TAA CCC - 3' and the strand Control with the sequence 5' - CTT TAA CAA ATA ATG ATA ATT - 3' was synthesized by IBA GmbH, Göttingen, Germany and labeled at the 3' end with Rhodamine Green (Molecular Probes, Eugene, OR) and a Thiol-C6 spacer at the 5'-end.
Sample preparation:
The surface was prepared for attachment as follows: 8 nm Au was deposited on glass coverslips (Superior, Marienfeld, Germany) by thermal evaporation. The coverslips were subsequently sputtered with Ar-Ions at 200 W, 7×10^{-7}mbar for 45 s, thus removing almost all Au from the surface. Afterwards, the coverslips were placed in 65% HNO_3 for 2 h. After rinsing with de-ionized water 1 μl droplets of 25μM DNA in PBS buffer containing 500 mM NaCl were spotted onto the coverslips and kept under 100% air moisture overnight. Then the coverslips were thoroughly rinsed with PBS and placed in PBS containing 10 mM Mercaptohexanol for 1/2 h to saturate the remaining Au-binding sites and remove unspecifically bound DNA. After rinsing with PBS the slides were ready for use.
Fluorescence microscopy:
The samples prepared as described above were mounted face up under a 200 μl PBS droplet on a object carrier on a fluorescence microscope (Olympus IX 71) and observed with a 10x objective. The images were recorded with a CCD camera (Photometrics CoolSnap HQ). To change the pH the samples were removed and rinsed under a buffer with the desired pH and placed again on the microscope under a 200 μl droplet of a buffer with the desired pH.

Chemical Oscillations:
The continuous stirred tank reactor consisted of two reservoirs, a reactor and two pumps (Minipuls 2, Gilson, Bad Camberg, Germany and XXS-EL20 E, thin xxs GmbH, Germany). Initially the cubic reactor contained 20 ml of Milipore water. One reservoir contained 19 mM $NaIO_3$. The other reservoir contained 30 mM Na_2SO_3, 21 mM $Na_2S_2O_3$, and 5 mM H_2SO_4. Both solutions were pumped at 150 μl/min into the reactor while the a second pump removed the excess volume at a speed of 300 μl/min. The reaction solution was constantly stirred at 150 rpm. After approximately 4 h the pH oscillation started and the glass-slide with the immobilized DNA strands were glued with silica-glue inside the reactor with the DNA facing the solution.
Energy transfer measurements:
For detection a modified fluorescence spectrometer (Jobin Yvon Fluorolog 3) was used: A 50/50 beam splitter was placed at the site normally used for the cuvette, guiding the excitation light (480 nm) through an objective (Leitz H32x/NA=0.60, WD=5.7 mm) onto the sample. The emitted light was collected through the same objective and reflected into the detection unit of the spectrometer with the beam splitter. The data was recorded with the spectrometer's software. The pH-value was measured and recorded simultaneously with a pH-Electrode (Schott, Mainz, Germany).

2. Formation of the i-motif in substrate-bound oligonucleotides

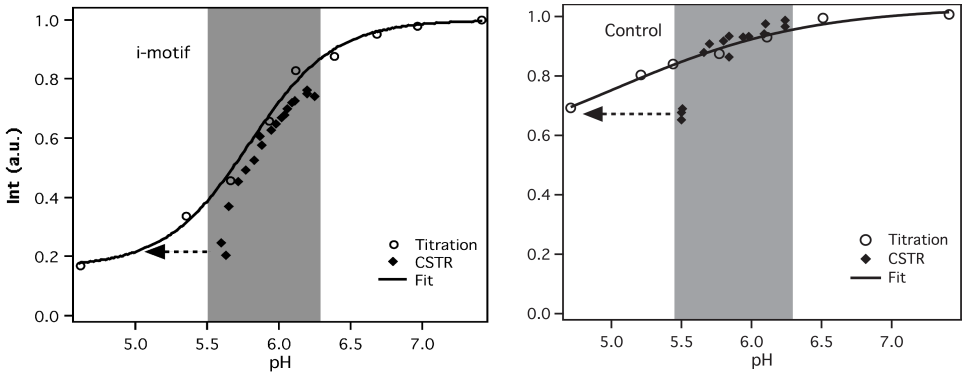

Figure 2: pH dependence of fluorescence of surface-bound labeled DNA strands. Left: The i-motif. Right: A control strand. The open symbols are data points recorded from a conventional titration while the closed symbols are directly taken from the device and control strand under the influence of the oscillator. Obviously, the behavior in the CSTR is consistent with that found in the titration experiment. The lowest fluorescence values recorded in the CSTR correspond to lower pH values than measured by the pH meter. As explained in the main text, this is due to the slowness of the response of the pH meter.

Fig. 2 shows the fluorescence of the i-motif and the control strand as a function of the pH value. Data marked with circles originate from a simple titration experiment where the pH in the solution surrounding the surface-bound DNA strands was altered by slowly adding HCl

and NaOH. The signal has been normalized to the value attained at pH 7.4. In case of the i-motif strand a strong increase of fluorescence can be observed around pH 6, whereas no such behavior is visible for the control strand. The sigmoidal shape (fit, solid line) of the curve, corresponding to strand M (the i-motif), may be explained by a cooperative transition to the other conformation, but at the same time it reflects the distance dependence of energy transfer between the dye and the gold/glass surface. The slight change in fluorescence for the control strand may reflect the protonation of adenine at low pH (adenine: $pK_a = 3.5$ and cytosine $pK_a = 4.2$), which results in an effective change of the charge of the DNA backbone which in turn reduces the electrostatic contributions to its persistence length. The same effect influences the cytosine rich i-motif, but it does not explain the sharp transition around pH 6. Data denoted by diamonds in Fig. S1 are obtained directly from a plot of the fluorescence intensity values against the pH taken from the CSTR experiments (Fig. 3 in the paper) for a few oscillation cycles. Both the i-motif and the control strand show the same pH dependence when driven by the pH oscillator as in the simple titration experiment. A few of these data points are "too low" when compared to the titration curve. As is argued in the paper, the pH values corresponding to these fluorescence intensities are actually lower than recorded by the pH-meter whose response time is too large too resolve the low pH spikes exhibited by the oscillator. These low pH spikes could be monitored, however, using the pH sensitive dye methyl orange which changes its color from yellow to pink between pH 4.4 and pH 3. This finding is also in agreement with the measurements of Rabai and Beck. Although the pH-dependence of Rhodamine Green is stated to be stable between pH 4 an pH 9, there is an effect on the fluorescence intensity of this dye below pH 4, which augments the uncertainty of the fluorescence data obtained for the low pH spikes.

To further confirm the formation of the i-motif by the surface-bound DNA strands M, temperature-dependent measurements were performed. A cuvette was filled with phosphate buffer (pH 5.8, 135 mM NaCl, 2.7 mM KCl), and 1 μM of DNA in case of the bulk measurements. The pH value of 5.8 was chosen near the transition point of the i-motif and was not altered during the experiments. When heating the cuvette a sharp increase in fluorescence is observed at $T = 37°C$ for the i-motif bound to the surface, while the control strand does not show any change in fluorescence under the same conditions (Fig. 4 in the paper). A DNA strand with the same sequence as the i-motif, but modified with a dye and a quencher on both ends shows a strong increase in fluorescence at slightly higher temperatures in a bulk experiment, whereas the fluorescence signal originating from an equally modified control strand does not change significantly. This is in agreement with previous circular dichroism measurements on the i-motif (G. Manzini, N. Yathindra, L. E. Xodo, Nucleic Acids Research, 1994, 22, 4634-4640).

For the energy transfer efficiency between a fluorescent dye and a gold surface, the distance dependence

$$E_T = \frac{1}{1 + (r/r_0)^4} \tag{1}$$

is expected. If one assumes energy transfer between dye and metal according to Yun et al. (Ref. 7c in the paper), the characteristic length r_0 is given by

$$r_0 = \left(\frac{0.525\ c^3 \Phi_D}{\omega^2 \omega_F k_F} \right)^{1/4}, \tag{2}$$

where ω_F and k_F are Fermi frequency and wavenumber of the metal, Φ_D and ω are the quantum efficiency and the fluorescence emission frequency of the dye, respectively. This

length is on the order of $9-10$ nm in our case. Due to a number of uncertainties, however, it is not easy to quantify the fluorescence data obtained in the experiments. A simple estimate would be that the distance between the fluorescent dye to the gold surface changes from roughly $0-1$ nm in the folded state to roughly 5 nm (the end-to-end distance for a random coil of single-stranded DNA with 22 nt) in the relaxed state. The latter distance may be considerably smaller, when the DNA strands make an angle with the surface, or larger when they are stretched, e.g., due to mutual repulsion.
Addition of the complementary strand increased the fluorescence signal in the case of the control strand but reproducibly decreased the signal for the i-motif at pH 8. Whereas the increased fluorescence for the control strand is easily explained by a stretching of the DNA due to duplex formation, and hence a larger distance of the fluorophore from the gold surface, it is not straightforward to explain the decrease in fluorescence for the i-motif strand. It is conceivable that due to the repetitive sequence of the i-motif strand the DNA molecules are crosslinked by the complementary strands, resulting in a reduced effective distance of the fluorophores to the surface. By the addition of a denaturing 8M solution of urea to the sample, the complementary strands can be removed and the fluorescence of both the i-motif and the control strand return to their original value.

3. pH dependence of fluorescence

Several effects influence the fluorescence recorded in our system: First of all, the dye Rhodamine Green is known to be pH insensitive between pH 4 and pH 9. Most of the time our system oscillates in this range but for fractions of a second the pH drops below pH 4 (compare text in paper) which makes an interpretation of fluorescence data obtained during these time intervals difficult. Another effect is the influence of the nucleobases on the fluorescence of a dye attached to a DNA strand (cf. C. A. M. Seidel et al., J. Phys. Chem., 1996, 100, pp. 5541-5553). The fluorescence intensity of a dye can be altered by photo-induced electron transfer which is dependent on the redox potential of the bases. This in turn is dependent on the pH value. As mentioned in the previous paragraph, protonation of one of the bases (adenine or cytosine) will also lead to a reduction of the overall charge of the oligonucleotides which will result in a reduced mean end-to-end distance. All these effects may in parts be responsible for the change in fluorescence of the control and the i-motif system, but they cannot account for the conformational transition of our device around pH 6 (Fig. S 2) and around 37°C (Fig. 4 in the paper). Plotting the fluorescence values obtained from the immobilized device and control strands under the influence of the oscillator (filled symbols in Fig. S2) show that the recorded fluorescence variations are consistent with the i-motif transition in the case of the device strand and with no such transition in the case of the control strand.

4. Modeling of the oscillatory reaction

For the oscillatory reaction, a solution of sodium iodate and a solution of sodium sulfite, sodium thiosulfite and sulfuric acid are continuously added to a reactor. The excess volume is removed at the same rate as it is pumped in. The dominant reactions taking place in the reactor are:

$$\mathrm{IO_3^- + 3\ HSO_3^- \rightarrow I^- + 3\ SO_4^{2-} + 3\ H^+}$$
$$\mathrm{IO_3^- + 5\ I^- + 6\ H^+ \rightarrow 3\ I_2 + 3\ H_2O}$$

$$\mathrm{IO_3^- + 6\ S_2O_3^{2-} + 6\ H^+ \rightarrow I^- + 3\ S_4O_6^{2-} + 3\ H_2O}$$
$$\mathrm{HSO_3^- \rightleftharpoons H^+ + SO_3^{2-}}$$

To model the pH oscillator we used the empirical kinetic model from the publications by Rabai and Beck (J. Phys. Chem. 92, 2804-2807 (1988); J. Phys. Chem. 92, 4831-4835 (1988)) for the Continuous stirred tank reactor (CSTR). With the abbreviations $j = [\mathrm{IO_3^-}] \times \mathrm{M}^{-1}$; $\mathrm{y} = [\mathrm{HSO_3^-}] \times \mathrm{M}^{-1}$; $\mathrm{s} = [\mathrm{SO_3^{2-}}] \times \mathrm{M}^{-1}$; $\mathrm{t} = [\mathrm{S_2O_3^{2-}}] \times \mathrm{M}^{-1}$; $\mathrm{h} = [\mathrm{H^+}] \times \mathrm{M}^{-1}$ the rate equations read:

$$\begin{aligned} v_1 &= k_{1a} jyh + k_{1b} jy^2 + k_c jyth^2 \\ v_2 &= k_2 y \\ v_{-2} &= k_{-2} sh \\ v_3 &= \frac{k_3 jt^2 h^2}{1 + k_i y} \end{aligned}$$

$$\begin{aligned} \frac{d}{dt}\, j &= -v_1 - v_3 + k_0(j_0 - j) \\ \frac{d}{dt}\, y &= -3v_1 - v_2 + v_{-2} - k_0 y \\ \frac{d}{dt}\, s &= v_2 - v_{-2} + k_0(s_0 - s) \\ \frac{d}{dt}\, t &= -6v_3 + k_0(t_0 - t) \\ \frac{d}{dt}\, h &= 3v_1 - 6v_2 + v_2 - v_{-2} + k_0(h_0 - h) \end{aligned}$$

$k_0 = 1.3 \times 10^{-3}\ \mathrm{s}^{-1}$ denotes the pump speed divided by the volume of the reactor. The other rate constants were chosen as follows: $k_{1a} = 8.8 \times 10^3\ \mathrm{s}^{-1}$; $k_{1b} = 18\ \mathrm{s}^{-1}$; $k_c = 1 \times 10^{11}\ \mathrm{s}^{-1}$; $k_2 = 30 \times 10^3\ \mathrm{s}^{-1}$; $k_{-2} = 5 \times 10^{10}\ \mathrm{s}^{-1}$; $k_3 = 3.4 \times 10^{12}\ \mathrm{s}^{-1}$; $k_i = 5 \times 10^4$. The inhibitory constant k_i is dimensionless. For the calculation for Fig. 3 in the paper and Fig. S3, the following intial conditions were chosen: $j(0) = 0$; $y(0) = 0$; $s(0) = 0$; $t(0) = 0$; $h(0) = 1 \times 10^{-7}$. The concentrations in the added reaction solution were $j_0 = 0.019$; $s_0 = 0.03$; $t_0 = 0.02$; $h_0 = 0.008$.

In the experiment, the reactor initially only contained water, the volume was 20 ml and was kept constant all over the time. The flow rate was 150 μl/min for both inlet tubes and 300 μl/min for the outlet tube. The values for the calculation are therefore close to the experimental conditions, albeit not identical. The very regular oscillations observed in the experiments can be well reproduced by this system of rate equations. Plugging in the pH dependence of the fluorescence of the DNA switches (from Fig. S1), one can plot the expected fluorescence curves (see Fig. 3 in the paper and Fig. S3). The rate equations were implemented and solved with a MATLAB (The MathWorks, Natick, MA) program on a personal computer.